Synthesis and Characterization of a New Aurivillius Phase

M.-L. Martínez-Sarrión,*[a] L. Mestres,[a] M. Herraiz,[a] A M. Balagurov,[b] A. I. Beskrovniy,[b] S. G. Vasilovskij,[b,c] and L. S. Smirnov[b]

Keywords: Aurivillius phase / Neutron diffraction / Solid-state structures / Perovskite phases

Several new Aurivillius phases with the general formula $Bi_{2.5+x}Li_{0.5-3x}Nb_2O_9$ ($0.04 < x < 0.08$) were synthesized. The crystal structure of the compound with $x = 0.04$ was studied by X-ray powder diffraction at room temperature, and by neutron powder diffraction in temperature intervals from 10 to 290 K. A single-phase compound was obtained. The crystal structure can be described by a space group, $Cmc2_1$, with lattice parameters of an orthorhombic unit cell: $a = 24.840(5)$ Å, $b = 5.449(6)$ Å, $c = 5.450(9)$ Å. The atomic positions were refined by a profile method. The conductivity of $Bi_{2.53}Li_{0.29}Nb_2O_9$ ranges from 1.35×10^{-8} S/cm at 543 K to 1.46×10^{-4}S/cm at 1013 K

Introduction

Aurivillius phases are described by the common formula $A_2O_2(A'_{n-1}B_nO_{3n+1})$,[1] where n denotes the thickness of the perovskite layers in terms of BO_6 octahedra. Currently, compounds are known with $n = 1$, 2, 3, 4, 5 and 8. Structures of this type show a great variability in their physical properties upon substitution of different metal cations.[2] This opens up great possibilities in the synthesis of new materials.

Some Aurivillius phases exhibit pseudo-tetragonal symmetry crystallizing in orthorhombic space groups. A large number of Aurivillius phases have been structurally characterized and all of them have tetragonal or pseudo-tetragonal symmetry, with a_o ranging between 3.85 and 3.95 Å ($a_{orthorhombic} = 5.45-5.58$ Å).[3]

The Aurivillius phases Bi_2WO_6, $Bi_2SrTa_2O_9$ and $Bi_4Ti_3O_{12}$ have been known as ferroelectric materials since the work of Smolenski et al.[4] and Subbarao,[5] who extensively studied their ferroelectrical properties as a function of composition. Thin films of $Bi_2SrTa_2O_9$ have been used in the recent developments in nonvolatile computer memory applications, such as an information storage medium.

The work of Withers and co-workers[6,7] has suggested that the major cause of spontaneous polarisation in the two-layer materials is the displacement of the A site cation in the perovskite block along the *a*-direction in the polar space group $A2_1am$ and not the movement of the B site cation away from the octahedral centre. A further important question regards the possibility of anti-site defects in the cation sublattice, Bi on the A site and A on the Bi site in the system $Bi_2ATa_2O_9$ (A = Ba, Sr, Ca; B = Nb, Ta). Recent work by Ismunandar et al.[8] using powder neutron diffraction data suggests that there is no cation-site disordering in these systems, although a similar study of $Bi_2PbNb_2O_9$ by Srikanth[9] suggests that some disorder may be present.

Blake et al.[10] used simultaneous X-ray and neutron powder refinements to obtain accurate models of the structure of $Bi_2BaNb_2O_9$, which is tetragonal with space group $I4/mmm$, and the structures of $Bi_2SrNb_2O_9$ and $Bi_2CaNb_2O_9$, which are orthorhombic with space group $Cmc2_1$. All the compounds exhibit disorder between the bismuth and A sites, increasing as the A-site cation size increases. The cause of this disorder may be explained by a combination of cation size considerations and bond valence sum analysis. It is possible that the two-layer Aurivillius structure may prefer a trivalent cation on the A site.

Durán-Martín and co-workers[11] have synthesised and characterised solid solutions $Bi_{2-x}Te_xSrNb_{2-x}B_xO_9$ (B = Zr, Hf) ($0 < x < 0.5$) and $Bi_{2-y}Te_ySr_{1-y}A_yNb_2O_9$ (A = K), ($0 < y < 0.25$). These materials are stable up to 800 °C for $y = 0.25$ and 750 °C for $x = 0.5$. All compositions are ferroelectric at room temperature. The AC electric conductivity shows anomalies at temperatures close to those where the remnant polarisation disappears.

In the last few years, some Aurivillius phases have been used as cathode materials in lithium batteries.[12,13] The aim of the present work is to investigate new Aurivillius phases with the general formula $Bi_{2.5+x}Li_{0.5-3x}Nb_2O_9$. These com-

[a] Departament de Química Inorgànica, Universitat de Barcelona, Martí i Franquès, 1−11, 08028 Barcelona, Spain
Fax: (internat.) + 34-934/907-725
E-mail: marialuisa.martinez@qi.ub.es
[b] Frank Laboratory of Neutron Physics, JINR, 141980 Dubna, Russia
[c] IP SB RAS, 660049 Krasnoayrsk, Russia

pounds have vacancies in the A-sites of the perovskite blocks that could promote the lithium mobility. The stoichiometry range, crystal structure and electrical behaviour have been studied.

Results and Discussion

Four compositions with general formula $Bi_{2.5+x}Li_{0.5-3x}Nb_2O_9$ ($0.04 < x < 0.08$), corresponding to an Aurivillius phase, were prepared. The use of powder XRD at room temperature confirmed that all the samples are monophasic with orthorhombic symmetry. Table 1 shows the formula and cell parameters for the new phases.

Table 1. Sample composition and cell parameters

	a (Å)	b (Å)	c (Å)	V (Å^3)
$Bi_{2.53}Li_{0.29}Nb_2O_9$	24.82(2)	5.440(6)	5.448(9)	735.59
$Bi_{2.54}Li_{0.24}Nb_2O_9$	24.81(1)	5.442(2)	5.457(1)	736.78
$Bi_{2.56}Li_{0.22}Nb_2O_9$	24.81(1)	5.444(2)	5.460(1)	737.46
$Bi_{2.59}Li_{0.20}Nb_2O_9$	24.81(1)	5.448(4)	5.458(2)	737.73

In order to understand these compounds better, $Bi_{0.53}Li_{0.29}Nb_2O_9$ was studied by neutron diffraction at different temperatures. Figure 1 shows the X-ray and neutron powder diffraction patterns at room temperature and also shows the initial indexing of the peaks. The figure shows that only the space group $Cmc2_1$ describes all the observed peaks. The atomic positions determined for $Bi_2CaNb_2O_9$ and $Bi_2SrNb_2O_9$ [10] were used as an initial model for Rietveld refinement.

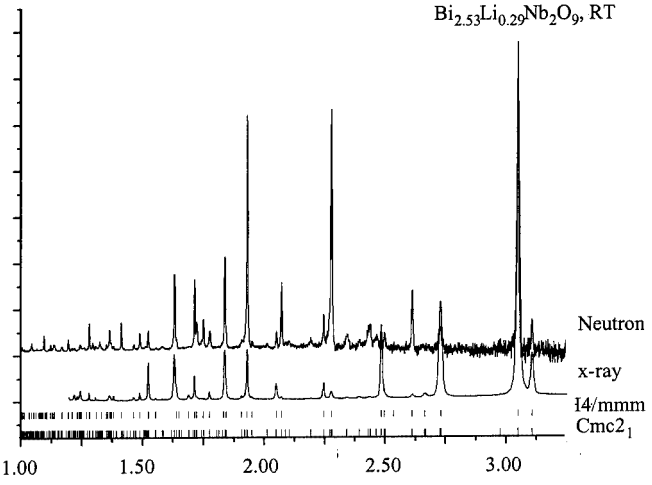

Figure 1. X-ray and neutron diffraction patterns at room temperature and initial indexing of the peaks for tetragonal *I*4/*mmm* and orthorhombic $Cmc2_1$ symmetry

Table 2 and 3 show the determined elementary cell parameters, the position of the atoms in the structure, the sites and the thermal factors in the isotropic approach, at 10 K and 290 K respectively.

Table 2. Crystallographic data for $Bi_{2.53}Li_{0.29}Nb_2O_9$ at 10K

Atom	Site	x	y	z	g	B_{iso}, Å^2
Bi(1)	4a	0.5	0.714(2)	0.274(4)	0.53	0.5
Li(1)	4a	0.5	0.546(1)	0.219(1)	0.29	0.5
Bi(2)	8b	0.2992(1)	0.7484(8)	0.258(1)	2.0	0.5
Nb	8b	0.4159(1)	0.255(1)	0.281(1)	2.0	0.2
O(1)	4a	0.5	0.208(2)	0.344(2)	1.0	0.5
O(2)	8b	0.3418(2)	0.307(1)	0.306(2)	2.0	0.5
O(3)	8b	0.7512(2)	0.506(1)	0.505(2)	2.0	0.5
O(4)	8b	0.4347(2)	0.531(1)	0.512(2)	2.0	0.5
O(5)	8b	0.4135(2)	0.053(1)	0.599(1)	2.0	0.5

R_{exp} (%) 7.7
R_p (%) 9.5
R_{wp} (%) 6.3
χ^2 3.4
Space group: $Cmc2_1$; a = 4.84373 ± 0.0019 Å, b =5.44599 ± 0.0005 Å, c =5.45467 ± 0.0005 Å

Table 3. Crystallographic data for $Bi_{2.53}Li_{0.29}Nb_2O_9$ at 290K

Atom	Site	x	y	z	g	B_{iso}, Å^2
Bi(1)	4a	0.5	0.729(2)	0.239(2)	0.53	2.65 ± 0.12
Li(1)	4a	0.5	0.694(8)	0.24(1)	0.29	1.01 ± 0.93
Bi(2)	8b	0.3000(1)	0.741	0.256(7)	2.0	2.15 ± 0.02
Nb	8b	0.4158(6)	0.2555(7)	0.2787(8)	2.0	1.76 ± 0.03
O(1)	4a	0.5	0.200(1)	0.334(1)	1.0	3.07 ± 0.09
O(2)	8b	0.3431(1)	0.3098(6)	0.312(9)	2.0	1.82 ± 0.05
O(3)	8b	0.7509(1)	0.508(6)	0.520(1)	2.0	1.61 ± 0.03
O(4)	8b	0.4325(1)	0.5326(8)	0.517(1)	2.0	3.55 ± 0.06
O(5)	8b	0.415(1)	0.0472(6)	0.5987(8)	2.0	2.52 ± 0.07

R_{exp} (%) 8.3
R_p (%) 12.5
R_{wp} (%) 7.3
χ^2 5.7
Space group:$Cmc2_1$; a = 24.849 ± 0.001 Å, b = 5.4536 ± 0.0003 Å., c = 5.4619 ± 0.0002 Å

At T = 10 K all the B_{iso} values are fixed. The results of the Rietveld refinement are shown in Figure 2. The observed neutron diffraction data are shown as a dotted line and the calculated profile as a solid line. A mark below the profile indicates the position of an allowed reflection. The lowest line near zero corresponds to the differences between observed and calculated intensities.

The possible variant of the replacement of bismuth by lithium in the bismuth oxide layer was checked during specification of the crystal structure. According to our calculations, the population of lithium in the bismuth oxide layer was nil. The bismuth oxide layer is much more inert with regard to substitution than the perovskite layer.[14,15] These data provide a basis for assuming that replacement of a bivalent ion in $Bi_2SrNb_2O_9$ or $Bi_2BaNb_2O_9$ by trivalent bismuth results in the formation of structural vacancies in the perovskite layer. The partial occupation of these vacancies

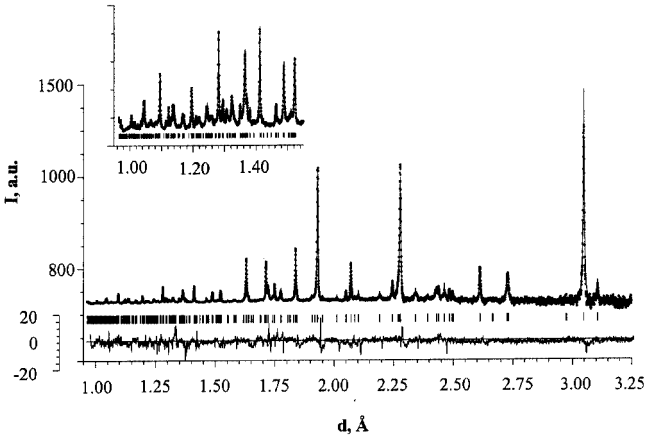

Figure 2. Observed, calculated (upper curve) and difference (lower curve) neutron profiles for $Bi_{2.53}Li_{0.29}Nb_2O_9$ obtained with an HRFD diffractometer at 290 K

by lithium ions can create favourable conditions for the development of ionic conductivity on structural vacancies.

The valences V_{ij} of the different cations were calculated from the atomic coordinates and Equation (1) (bond valence method):

$$V_{ij} = \sum_{i}^{v} s_{ij}\left(R_{ij}\right) \quad (1)$$

where v is the coordination number.

The dependence of valence strain s_{ij} on the bond length R is determined as:

$$s_{ij} = \exp\left[\left(R_{1j} - R_{ij}\right)/b\right] \quad (2)$$

where R_1 is the bond length of the individual valence, and the empirical parameter b is 0.37 Å (Table 4).

Table 4. Calculated valency for cations

Atom	Bond valence		
	T = 10 K	T = 290 K	Model
Bi	3.03	2.89	3
(Bi/Li)	1.89	1.81	1.88
Nb	4.94	5.14	5

The arrangement of octahedra in the structure is distorted. There is also a noticeable distortion of their form. Table 5 gives the bond lengths between atoms that fall into an octahedral configuration.

Table 5. Bond lengths in the NbO_6 octahedra

Bond type	L, Å	
	T = 10 K	T = 290 K
Nb−O(1)	2.131	2.136
Nb−O(2)	1.868	1.831
Nb−O(4)	1.925	1.882
	2.019	2.039
Nb−O(5)	1.957	1.992
	2.054	2.085

In order to gain a better understanding of this compound powder neutron diffraction data were collected at high temperature on a DN-2 diffractometer. On the basis of these data, the dependence of the parameters of an elementary cell on the temperature were deduced (Figure 3). From the given dependences it may be seen that orthorhombic distortion of the structure increases with temperature. This is not consistent with the data, which are given for $Bi_2(Sr, Ca)Nb_2O_9$.[10]

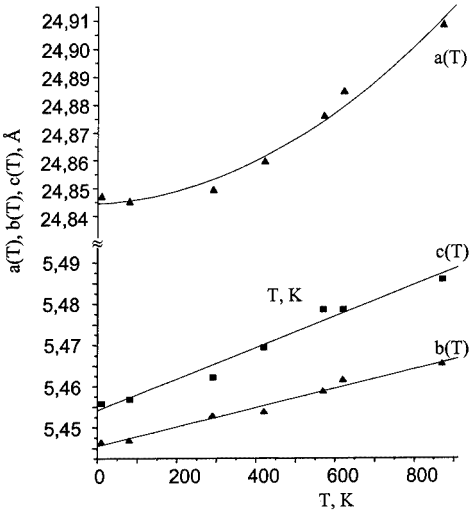

Figure 3. Dependence of the elementary cell parameters of $Bi_{2.53}Li_{0.29}Nb_2O_9$ vs. temperature

The plot of the parameters against temperature in Figure 3 shows a possible phase transition between 600 and 650 K. The small structure distortion due to the presence of lithium in the 12-coordinated positions of the perovskite part would lead to a possible phase transition at high temperature, in agreement with the small change in the slope observed in the plot.

Analysis of the results of TG and DSC analysis did not show the presence of a phase transition of these compounds in our experimental conditions, although one has to take into account that not all phase transitions carry an enthalpy variation detectable by DSC.

Figure 4 shows the structure of the new Aurivillius phase $Bi_{2.53}Li_{0.29}Nb_2O_9$, which may be described structurally as intergrowths of fluorite-like $Bi_2O_2^{2+}$ layers with perovskitic $(A'_{n-1}B_nO_{3n+1})^{2-}$ layers (n = 2). The $Bi_2O_2^{2+}$ layers are composed of a square planar net of oxygen anions with Bi^{3+} in an alternating sequence above and below, forming BiO_4-pyramids. Double perovskite layers are inserted between $Bi_2O_2^{2+}$ layers. Nb^{5+} cations are on the B-site, and Bi^{3+}, Li^+ and vacancies can be found on the A′ positions. NbO_6 octahedra in the structure are partially collapsed as a result of a cooperative tilting and rotating due to the presence of Bi^{3+}, Li^+ and vacancies placed on the larger A′ sites of the perovskite structure.

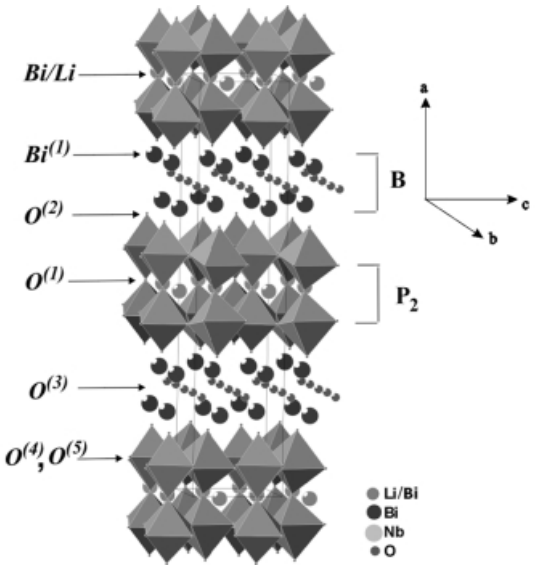

Figure 4. Crystal structure of $Bi_{2.53}Li_{0.29}Nb_2O_9$; octahedra NbO_6: large black spheres, Bi: small grey spheres O; large grey balls are Bi, Li or vacancies

AC impedance measurements were carried out on sintered pellets (diameter ≈ 6 mm and thickness ≈ 2 mm) of the sample $Bi_{2.53}Li_{0.29}Nb_2O_9$, using gold electrodes. The conductivity was measured up to 750 ΘC, the maximum temperature allowed by our sample holders. An almost perfect semicircle associated with the bulk conductivity (C ≈ 40pF) was observed (Figure 5) and the conductivity was determined from the intercepts on the real axis.

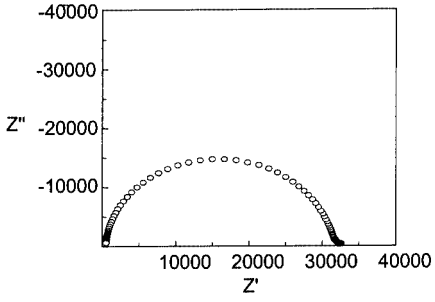

Figure 5. Impedance spectra for $Bi_{2.53}Li_{0.29}Nb_2O_9$ at 953 K

Figure 6 shows the variation of the dielectric constant (ε′) as a function of the temperature for different frequencies during the heating run. As can be seen, there are two anomalies in the behaviour of this constant; the first one at approximately 573 K and the second one at 873 K. The maximum corresponding to the first one shifts to lower temperatures with decreasing frequency. This kind of behaviour of the dielectric constant is typical of materials with a diffuse phase transition, and is also found for different ferroelectric materials.[17,18] For temperatures above 873 K a further increase of the dielectric constant was observed as the increasing electric conductivity leads to a dielectric breakdown.[19]

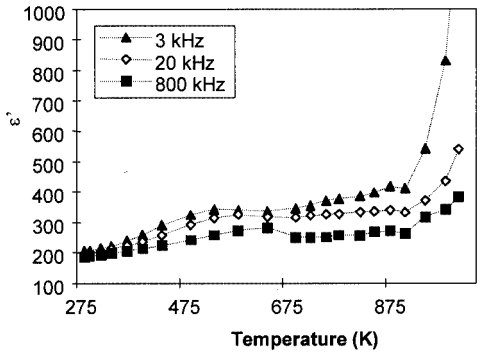

Figure 6. Dielectric constant ε′ of $Bi_{2.53}Li_{0.29}Nb_2O_9$ vs. temperature for different frequencies

Conductivity data from the impedance complex plane plots are shown in Arrhenius format in Figure 7. The plot is not linear and the slope changes around the same temperatures where the dielectric permittivity plots show anomalies that may be attributed to a phase transition. The activation energy changes from 0.57 eV to 0.93 eV, and finally 1.43 eV.

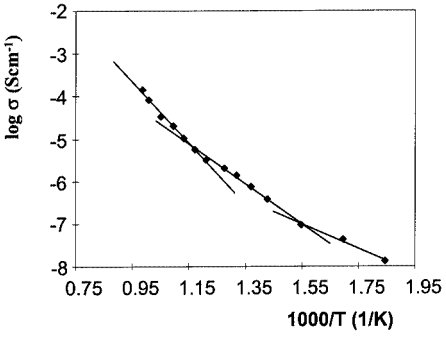

Figure 7. Arrhenius plots of conductivity for $Bi_{2.53}Li_{0.29}Nb_2O_9$

Experimental Section

Synthesis: Samples were prepared in 10 g quantities from Bi_2O_3 (Aldrich 99.9%), Li_2CO_3 (Aldrich, purity > 99.0%) and Nb_2O_5 (Aldrich 99.9%). Nb_2O_5 was dried overnight at 950 °C prior to weighing. These chemicals were weighed, mixed in an agate mortar with acetone, dried and heated to 650 °C for 3 h to drive off CO_2. After grinding, samples were pressed into pellets and covered with powder of the same composition to avoid loss of lithium during thermal treatment. The pellets were fired at 950 °C for 4 h yielding white products, which were reground, re-pelleted and fired at 1025 °C for 12 h and at 1100 °C for 6 h.

Analysis: Lithium, bismuth and niobium stoichiometries were obtained by ICP with a Jovin Ivon instrument.

X-ray Diffraction: Phase purity was checked by X-ray powder diffraction with a Siemens D-500 diffractometer in reflection mode and a secondary monochromator using Cu-K_α radiation. The program FULLPROF was used for Rietveld refinements.[20]

Neutron Diffraction: Neutron diffraction experiments were carried out in the FLNP, JINR at the IBR-2 pulse reactor using two different diffractometers. On the DN-2 diffractometer, the neutron dif-

fraction data were measured in the range from 1.5 Å to 12 Å at medium resolution. On the HRFD diffractometer, neutron diffraction data were recorded in the range from 1 Å to 3.2 Å at high resolution. The unit-cell parameters were determined using the AUTOX program for automatic indexing.[21] The atomic positions were refined by the Rietveld profile analysis using the MRIA program.[22]

Thermal Analysis: The thermal analysis for the temperature range 298−1173 K by thermogravimetry (TG), and from 123−873 K by differential scanning calorimeter (DSC) was carried out in a Mettler Toledo Star System. With TG the warming rate was 10 K/min, and the weight of the sample, was 27.4027 mg. In the DSC study the weight of the sample was 12.2430 mg from 298 K to 873 K, and 12.8800 mg, from 123 K to 298 K. The measurements were made during both heating and cooling. The reference material was alumina.

Electrical Measurements: AC measurements were carried out using a HP 4192A Impedance Analyser over the range100 Hz $< f <$ 1.3 $\times$ 10^7 Hz. Data corrections were carried out in order to avoid the stray capacitance of the jig and the stray inductance and series lead resistance associated with the leads; data above 5 $\times$ 10^6 Hz were discarded.

Acknowledgments

This work was partially sponsored by financial support from 99-SGR-00044 and INTAS-97-10177.

[1] B. Aurivillius, *Ark. Kemi* **1949**, *1*, 465−480.
[2] K. S. Aleksandrov, B. V. Beznosikov, *Crystals of Type Perovskite*, "Saince", Novosobirst, **1999**.
[3] J. F. Ackerman, *J. Solid State Chem.* **1986**, *62*, 92−104.
[4] G. A. Smolenski, V. A. Isupov, A. I. Agranovskaya, *Sov. Phys. Solid. State (Engl. Transl.)* **1959**, *3*, 651.
[5] E. C. Subbarao, *J. Phys. Chem. Solids* **1962**, *23*, 665−676.
[6] A. D. Rae, J. G. Thompson, R. L. Withers, *Acta Crystallogr., Sect. B* **1992**, *48*, 418−428.
[7] R. L. Withers, J. G. Thompson, A. D. Rae, *J. Solid State Chem.* **1991**, *94*, 404−417.
[8] Ismunandar, B. J. Kennedy, Gunawan, Marsongkohadi, *J. Solid State Chem.* **1996**, *126*, 135−141.
[9] V. Srikanth, H. Idink, W. B. White, E. C. Subbarao, H. Rajagopal, A. Sequeira, *Acta Crystallogr., Sect. B* **1996**, *52*, 432−439.
[10] S. M. Blake, M. J. Falconer, M. McCreedy, P. Lightfoot, *J. Mater. Chem.* **1997**, *7*, 1609−1613.
[11] P. Durán-Martín, B. Jiménez, P. Millán, A. Castro, *J. Phys. Chem. Solids* **2000**, *61*, 1423−1431.
[12] M. E. Arroyo y de Dompablo, F. García-Alvarado, E. Morán, *Solid State Ionics* **1996**, *91*, 273−278.
[13] J. H. Choy, J. Y. Kim, I. Chung, *J. Phys. Chem. B* **2001**, *105*, 7908−7912.
[14] A. Castro, P. Millán, M. J. Martínez-Lopez, *Solid State Ionics* **1993**, *63−65*, 897−901.
[15] P. Millán, A. Castro, J. B. Torrance, *Mater. Res. Bull.* **1993**, *28*, 117−122.
[16] V. S. Urusov, I. P. Orlov, *Crystallogr. Rep.* **1999**, *44*, 686−709.
[17] L. E. Cross, *Ferroelectric Ceramics: Tailoring Properties for Specific Applications*, Birkhäuser, Basel, **1993**.
[18] M. E. Lines and A. M. Glass, *Principles and Applications of Ferroelectrics and Related Materials* Oxford University Press, Oxford, **1977**.
[19] H. M. Rosenberg, *The Solid State* Oxford University Press, Oxford, **1988**.
[20] J. Rodríguez Carvajal, "Fullprof: A program for Rietveld refinement and pattern machine analysisi," revised version, 1994.
[21] V. B. Zlokazov, *Comput. Phys. Commun.* **1995**, *85*, 415−422.
[22] V. B. Zlokazov, V. V. Chernyshev, *J. Appl. Crystalogr.* **1992**, *25*, 447−451.

Received November 29, 2001
[I01487]